Spin Injection and Relaxation in a Mesoscopic Superconductor

N. Poli,[1] J. P. Morten,[2] M. Urech,[1] Arne Brataas,[2] D. B. Haviland,[1] and V. Korenivski[1]

[1]*Nanostructure Physics, Royal Institute of Technology, 10691 Stockholm, Sweden*
[2]*Department of Physics, Norwegian University of Science and Technology, 7491 Trondheim, Norway*

We study spin transport in a superconducting nanowire using a set of closely spaced magnetic tunnel contacts. We observe a giant enhancement of the spin accumulation of up to 5 orders of magnitude on transition into the superconducting state, consistent with the expected changes in the density of states. The spin relaxation length decreases by an order of magnitude from its value in the normal state. These measurements, combined with our theoretical model, allow us to distinguish the individual spin-flip mechanisms present in the transport channel. Our conclusion is that magnetic impurities rather than spin-orbit coupling dominate spin-flip scattering in the superconducting state.

The nonlocal measurement technique [1] is a powerful way to directly probe nonequilibrium spin populations. The technique has been used to uncover a number of spin-dependent phenomena in nanostructures, such as electron spin precession [2], spin Hall effect [3], and spin injection and propagation in Si [4] and graphene [5]. Experiments reported to date have focused on normal metals and semiconductors. In this Letter, we present direct measurements of the spin transport parameters in a superconductor, performed using a multielectrode nanodevice with tunnel junction injection and simultaneous spin-sensitive detection at different mesoscopic distances from the injection point. We observe dramatic changes in the properties of the injected nonequilibrium spins on transition of the nanowire into the superconducting state. An interpretation of the observed effects is given by extending recently developed theories [6–10].

Nonequilibrium superconductivity has been studied since the pioneering experiments on tunnel injection of quasiparticles (QPs) into superconductors (S) from normal (N) and ferromagnetic (F) metals [11,12]. It was found that the injected electrons remain unpaired QPs for about 10 μs before they combine to form Cooper pairs and condense in the superconducting ground state [13,14]. The first experimental study on *spin-dependent* injection and detection in superconductors (Nb) using a nonlocal measurement configuration indicated a strong reduction in the spin-flip length (λ_{sf}) at $T < T_c$ [15]. On the other hand, local measurements on metal stacks containing Nb were used to infer only a small reduction in λ_{sf} on transition into the superconducting state [16]. A twofold decrease in λ_{sf} of Al below T_c was estimated by studying injection from ferromagnetic metals into superconductors and using *spin-independent* detection [17]. All of these experiments on spin injection and relaxation in superconductors used metallic contacts between the ferromagnetic electrodes and the superconductor, which is known to lead to proximity effects suppressing the gap in superconductors and strong Andreev processes [18]. Furthermore, λ_{sf} was not mea-

sured directly as the magnitude of spin splitting in superconductors vs the distance from the spin injection point, but rather inferred from the charge transport characteristics. Our device allows us to simultaneously measure the spin splitting at several points along the superconducting nanowire, and thereby directly determine λ_{sf} in superconductors, without the complications due to the proximity effects or Andreev processes.

Figure 1(a) shows a scanning electron microscopy (SEM) image of our device, together with a schematic of the measurement arrangement, which is an extension of the configuration first used by Johnson and Silsbee [1]. The samples were fabricated using *e*-beam lithography and a two-angle deposition technique. For the details of the fabrication process and magnetic characterization, see [19–21]. A set of Co/Al-O/Al tunnel junctions closely spaced along the nanowire of Al were formed. Not only does the use of tunnel junctions increase the effective spin polarization and thereby the spin signal to be detected [22], it is also important in providing true QP injection and suppressing Andreev reflection effects.

Injecting spin-polarized charge current from the ferromagnetic electrodes into the Al nanowire induces a spin accumulation, which decays away from the injection point due to spin relaxation, as shown in Fig. 1(b), with the spatial profile governed by the diffusion equation [Eq. (2) of Ref. [8]]. The voltage difference taken between the parallel (P) and the antiparallel (AP) magnetic states of the injector/detector, normalized by the current, defines the nonlocal spin signal, which in the normal state is given by [1,2,8]

$$R_S(x) = \frac{V_P - V_{AP}}{I_{inj}} = P^2 R_N \exp(-x/\lambda_{sf}), \qquad (1)$$

where P is the spin polarization, $R_N = \rho \lambda_{sf}/A$ is the characteristic resistance of normal metals, ρ is the resistivity of Al, and A is the cross sectional area of the Al strip. $\lambda_{sf} = \sqrt{D\tau_{sf}}$ is the spin-flip length, D is the diffusion constant, and τ_{sf} is the spin-flip time.
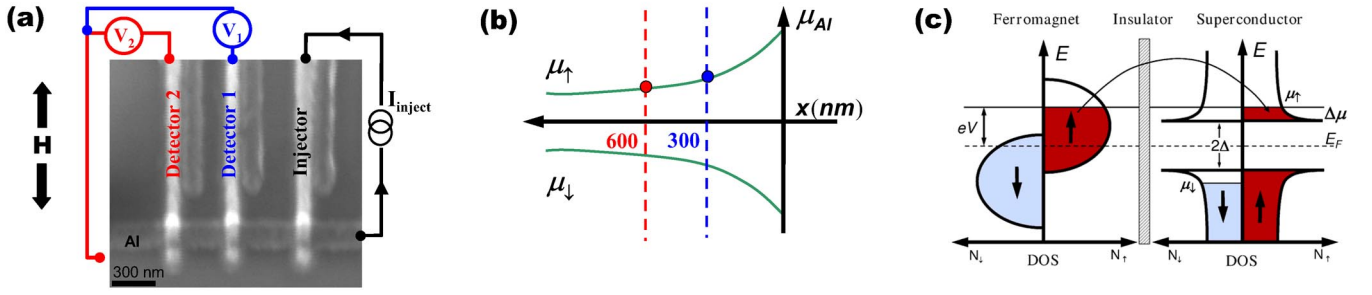
FIG. 1 (color online). (a) SEM image of the sample together with the nonlocal measurement configuration. The electrical circuit schematic illustrates the measurement arrangement used for directly measuring λ_{sf}. (b) λ_{sf} is the exponential decay length of the spin accumulation away from the injection point. (c) Schematic density of states, illustrating spin accumulation ($\Delta\mu = \mu_\uparrow - \mu_\downarrow$) due to tunneling between a ferromagnet and a superconductor.

A number of novel effects connected with spin injection and relaxation in superconductors have been predicted recently [6–10]. Cooper pairs have zero spin and carry only charge. It is therefore spin-polarized electrons tunneling into the QP branches that transport spin in superconductors. Figure 1(c) illustrates the spin accumulation ($\mu_\uparrow - \mu_\downarrow$) in superconductors due to spin-polarized tunneling from ferromagnetic metals. Observe that the minimum injection energy is the gap energy in the superconductor $\Delta \approx 200 \ \mu$eV for Al. If the injection energy is close to the gap energy (Δ), then spin-polarized QPs can be created and charge imbalance avoided [23]. A dramatic increase in the spin accumulation compared to that in the normal state for the same injection current and near-gap bias is then expected [8]. This is understood as originating from the reduction in the density of states of the QPs due to the opening of the gap in the energy spectrum. Considering spin relaxation due to spin-orbit interaction, the proper spin signal in superconductors is obtained by scaling R_N in Eq. (1) with the density factor $[2f_0(\Delta)]^{-1}$ [8]:

$$R_S(x) = P^2 \frac{R_N}{2f_0(\Delta)} \exp(-x/\lambda_{sf}), \qquad (2)$$

where $f_0(E) = 1/[\exp(E/kT) + 1]$ is the Fermi distribution function for a given temperature T. Thus, a diverging spin signal is expected in superconductors as $T \rightarrow 0$.

More generally, relaxation of the above nonequilibrium spin accumulation in superconductors is governed by two main mechanisms: scattering by spin-orbit interaction and magnetic impurities. In the elastic limit, these two mechanisms have been studied theoretically and are expected to result in a different energy and temperature dependence of the spin-flip processes [9,10]. Hence, λ_{sf} becomes an energy and temperature dependent quantity in the superconducting state and cannot be quantified by a number, but rather by a function. Seemingly a complication, this $\lambda_{sf}(T)$ dependence can be used to distinguish between the different spin relaxation mechanisms in our device, thus leading to a novel spin-flip spectroscopy. The specific prediction is that spin-flip by magnetic impurities is enhanced for QP energies close to Δ, whereas spin-flip due to spin-orbit

interaction is the same in superconducting and normal metal states. We assume that the spectral properties of the aluminum are given by the spatially homogeneous BCS solutions with the temperature dependence of the gap $\Delta \approx 1.76 T_C \tanh(1.74\sqrt{T/T_C - 1})$, where $t = T/T_C$ is the normalized temperature. This assumption is valid when the contacts to the superconductor are of low transparency and of spatial dimensions smaller than the coherence length in superconductors—the geometry chosen in this experiment with ~50 nm scale tunnel contacts. In the linear response limit, the nonlocal spin signal at the detector contact at a distance x away from the injection point becomes

$$R_S(x) = P^2 R_N \frac{g(x/\lambda_{sf}, t)}{\chi(t)h(t)}, \qquad (3)$$

where $\chi(t) = -2 \int_\Delta^\infty \frac{E}{\sqrt{E^2 - \Delta^2}} \frac{\partial f_0(E)}{\partial E} dE$ is the Yosida function, and $g(x/\lambda_{sf}, t)$ and $h(t)$ are rather complex energy integrals that can be approximated in superconductors as $h(t) \approx (1 - P^2)\chi(t)$ and

$$g(x/\lambda_{sf}) \approx \int \frac{\partial f_0(E)}{\partial E} \frac{-4N^2(E)e^{-x/(\lambda_{sf}\alpha)}}{2\alpha + N(E)R_N/R_I} dE. \qquad (4)$$

Here R_I is the injector tunnel resistance, $N(E)$ is the density of states of the superconductor, and $\alpha = \sqrt{(E^2 - \Delta^2)/(E^2 + \beta\Delta^2)}$ gives the renormalization of λ_{sf}. The parameter $\beta = (\tau_{so} - \tau_m)/(\tau_{so} + \tau_m)$, with τ_{so} and τ_m being the normal state spin orbit and magnetic impurity spin relaxation times, respectively, is a measure of the relative contributions from the two scattering mechanisms. β is expected to approach 1 if magnetic impurities dominate spin-flip processes, i.e., $\tau_m \ll \tau_{so}$, which results in a substantial decrease in λ_{sf}. For dominating spin-orbit induced spin-flip, i.e., $\tau_m \gg \tau_{so}$, $\beta = -1$ which gives $\alpha = 1$, so that there is no renormalization of λ_{sf} in Eq. (3). The effective λ_{sf} can be extracted by fitting the theoretical R_S of Eq. (3) to the R_S measured by the two detectors placed at 300 and 600 nm.

The multielectrode nanodevice discussed above and illustrated in Fig. 1(a) is capable of direct measurements

of the spin accumulation and the spin-flip length and is, therefore, ideal for exploring the fundamental properties of spin transported in superconductors. Measuring the spin signal vs the distance, x, from the injection point, as shown in Fig. 1(b), allows a direct determination of the spin-flip length, λ_{sf}. In our case of multiple spin detectors, this direct measurement of λ_{sf} is done *in situ* in the same device, in a single field sweep. The measurements were performed using the lock-in technique, with a 7 Hz bias signal applied to the injector and the right end of the Al wire. Typical values of the bias current used were $I_{inject} = 5$ μA rms in the normal metal state and 1–10 nA in the superconducting state of the nanowire. The nonlocal voltages V_1 and V_2 were measured using preamplifiers with very high input impedance ($\sim 10^{15}$ Ω) and low input bias currents (~ 10 fA) in order to minimize spurious contributions to the detected signals. At 4 K the typical junction resistance is 50–200 kΩ with a resistance area product of ~ 1 kΩ μm^2. The resistivity of the thin Al is 5–10 $\mu\Omega$ cm. Using the Einstein relation $\sigma = e^2 N_{Al} D_N$, with $N_{Al} = 2.4 \times 10^{28}$ eV^{-1} m^3 [2] being the density of states at the Fermi level, gives the diffusion constant $D_N = (3-9) \times 10^{-3}$ m^2 s^{-1}. Fitting the data from typical R_S vs H (applied magnetic field) curves [20,21] to Eq. (1) yields $\lambda_{sf} = 800-1100$ nm, $\tau_{sf} \approx 100$ ps and the effective spin polarization of $P = 12\%$. These spin transport parameters in the normal metal state are in good agreement with the recent results for similar structures [2,3,24,25].

It is important that the spin channel remains superconducting throughout the magnetotransport measurements. The typical bias current used for the transport measurements in the superconducting state is ~ 1 nA, which is low enough not to suppress superconductivity due to QP injection. Moreover, from critical current measurements, similar to those reported previously [21], we conclude that possible changes in the fringing fields have no effect on the superconducting parameters relevant for the spin transport properties discussed below.

Figure 2 shows the normalized R_S for sample 1 for $x = 300$ nm as a function of temperature. The bias current was kept at 1 nA in order not to affect the superconducting gap by the QP injection [21], and to obtain near-gap injection energies. R_S is enhanced in the superconducting state by 4 to 5 orders of magnitude. This is by far the largest R_S measured in a metal-oxide nanostructure. The theoretical fit using Eqs. (3) and (4) approximates well the experimental data for temperatures down to $T \sim 0.2 T_C$, at which point the measured R_S starts leveling off. We believe this to be due to an effective QP temperature higher than that given by the thermometer in the 10–100 mK range [26]. The QPs are relatively decoupled from the phonon bath at the lowest temperatures. The noise due to the electromagnetic environment in the measurement system affects the injected QPs and raises their temperature. This heat is not fully dissipated by the phonon bath, since the phonon population vanishes as T approaches zero. In order to
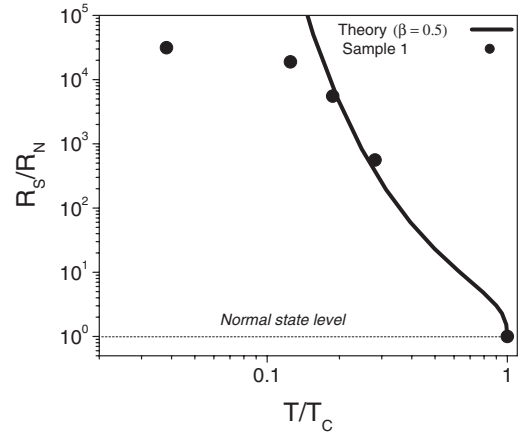

FIG. 2. Normalized spin signal (R_S) for sample 1, as a function of normalized temperature. $T_C \approx 1.6$ K and $R_S(4$ K$) \approx 50$ mΩ.

determine the effective QP temperature, we model the normalized differential conductance of the injection junction, measured at 22 mK. Using the model of [27], Fig. 3 shows the best fit, which was obtained for $T_{eff} \approx 0.2 T_C$. This value is consistent with the saturation behavior of R_S, further supporting our interpretation. Thus, the measured R_S saturates as $T \rightarrow 0$, but its dramatic enhancement of 4–5 orders of magnitude is a strong confirmation of the recent theoretical predictions on spin injection in superconductors [8,10].

Another key quantity determining spin transport in superconductors is the spin relaxation length, which can be used to differentiate the different spin relaxation mechanisms present in the device. Figure 4 shows the normalized λ_{sf} for two samples as a function of temperature. The critical temperature for both samples is $T_C \approx 1.6$ K and $\lambda_{sf}(T \gtrsim T_C) \approx 1$ μm. The measured λ_{sf} decreases substantially at low temperature, by a factor of 10 at 20 mK compared to its value in the normal metal state. This temperature dependence of λ_{sf} is inconsistent with the behavior predicted for pure spin-orbit scattering [6,8], but is in good agreement with the predictions for magnetic impurity mediated spin-flip [9,10]. The $\lambda_{sf}(T)$ data are well described by the theoretical dependence of Eq. (3), as shown in Fig. 4 by the solid line. The best fit was obtained
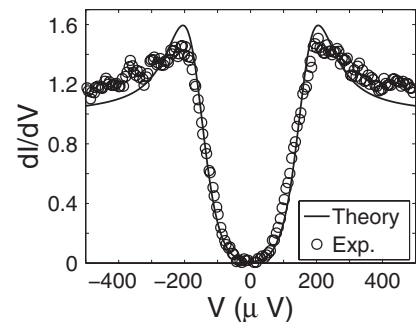

FIG. 3. Normalized differential conductance of the injection junction measured at 22 mK, together with a theoretical fit [27]. The best fit was obtained for $T_{eff} \approx 0.2 T_C$.
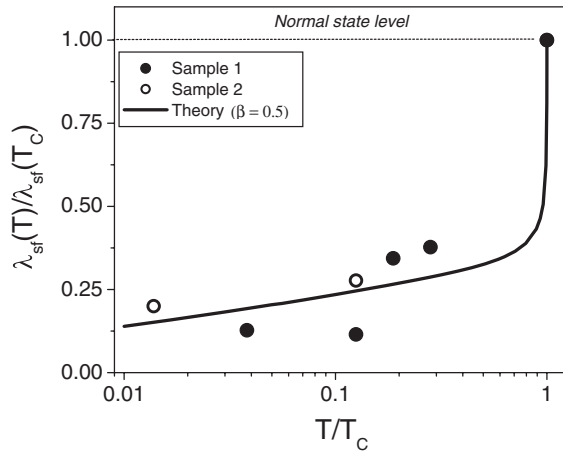
FIG. 4. Normalized spin diffusion length (λ_{sf}) for two samples, 20–25 nm in thickness, as a function of normalized temperature (T/T_C). $T_C \approx 1.6$ K and $\lambda_{sf}(4$ K$) \approx 1$ μm. The error bars (not shown) are approximately of the size of the symbols representing the data points.

for $\beta = 0.5$, which is equivalent to $1/\tau_m = 3/\tau_{so}$. This means that spin-flip scattering due to magnetic impurities is 3 times more likely than spin-flip by spin-orbit interaction. With $\beta = 0.5$ the renormalization of the scattering rates described by α yields a diverging spin-flip rate as T approaches zero, since the spins are injected close to the gap edge, where $\alpha \approx 0$.

A magnetic impurity concentration of $\sim1\%$ is known to suppress superconductivity [28–30], which would manifest in a reduced T_C. Our measured T_C is greater than that of pure Al due to nonmagnetic impurity scattering, typical for thin films (grain boundary and surface scattering). From this we estimate an upper limit on the concentration of magnetic impurities at 0.1%. Previous results show that even a magnetic impurity concentration of 0.005% can lead to a significant renormalization of λ_{sf} in the superconducting state [29]. Thus, the spin-flip rate can be significantly enhanced even for low concentrations of magnetic impurities.

In conclusion, we report direct measurements of the main parameters of spin transport in a superconductor. The mesoscopic multiterminal device used allows an *in situ* determination of the spin accumulation and the spin relaxation length of quasiparticles, which carry the spin current in the superconducting state. We observe a record high enhancement of the spin injection efficiency for near-gap bias, up to 4 to 5 orders in magnitude compared to the normal state, and an order of magnitude reduction in the spin relaxation length at $T \ll T_C$. These effects are explained theoretically as being due to changes in the quasiparticle density of states caused by opening of the superconducting gap, and strong enhancement in spin-flip scattering from magnetic impurities at energies close to the gap energy.

[1] M. Johnson and R. H. Silsbee, Phys. Rev. Lett. **55**, 1790 (1985).
[2] F. J. Jedema, H. B. Heersche, A. T. Filip, J. J. S. Baselmans, and B. J. van Wees, Nature (London) **416**, 713 (2002).
[3] S. O. Valenzuela and M. Tinkham, Nature (London) **442**, 176 (2006).
[4] I. Appelbaum, B. Q. Huang, and D. J. Monsma, Nature (London) **447**, 295 (2007).
[5] N. Tombros, C. Jozsa, M. Popinciuc, H. T. Jonkman, and B. J. van Wees, Nature (London) **448**, 571 (2007).
[6] H. L. Zhao and S. Hershfield, Phys. Rev. B **52**, 3632 (1995).
[7] T. Yamashita, S. Takahashi, H. Imamura, and S. Maekawa, Phys. Rev. B **65**, 172509 (2002).
[8] S. Takahashi and S. Maekawa, Phys. Rev. B **67**, 052409 (2003).
[9] J. P. Morten, A. Brataas, and W. Belzig, Phys. Rev. B **70**, 212508 (2004).
[10] J. P. Morten, A. Brataas, and W. Belzig, Phys. Rev. B **72**, 014510 (2005).
[11] J. Clarke, Phys. Rev. Lett. **28**, 1363 (1972).
[12] P. M. Tedrow and R. Meservey, Phys. Rev. B **7**, 318 (1973).
[13] J. L. Levine and S. Y. Hsieh, Phys. Rev. Lett. **20**, 994 (1968).
[14] S. Y. Hsieh and J. L. Levine, Phys. Rev. Lett. **20**, 1502 (1968).
[15] M. Johnson, Appl. Phys. Lett. **65**, 1460 (1994).
[16] J. Y. Gu, J. A. Caballero, R. D. Slater, R. Loloee, and W. P. Pratt, Jr., Phys. Rev. B **66**, 140507(R) (2002).
[17] Y. S. Shin, H. J. Lee, and H. W. Lee, Phys. Rev. B **71**, 144513 (2005).
[18] A. F. Andreev, Sov. Phys. JETP **19**, 1228 (1964).
[19] M. Urech, V. Korenivski, N. Poli, and D. B. Haviland, Nano Lett. **6**, 871 (2006).
[20] N. Poli, M. Urech, V. Korenivski, and D. B. Haviland, J. Appl. Phys. **99**, 08H701 (2006).
[21] M. Urech, J. Johansson, N. Poli, V. Korenivski, and D. B. Haviland, J. Appl. Phys. **99**, 08M513 (2006).
[22] E. I. Rashba, Phys. Rev. B **62**, R16 267 (2000).
[23] M. Tinkham and J. Clarke, Phys. Rev. Lett. **28**, 1366 (1972).
[24] S. Garzon, I. Zutic, and R. A. Webb, Phys. Rev. Lett. **94**, 176601 (2005).
[25] S. O. Valenzuela, D. J. Monsma, C. M. Marcus, V. Narayanamurti, and M. Tinkham, Phys. Rev. Lett. **94**, 196601 (2005).
[26] S. Corlevi, W. Guichard, F. W. J. Hekking, and D. B. Haviland, Phys. Rev. Lett. **97**, 096802 (2006). In related experiments using the same measurement system, the effective QP temperature due to the electromagnetic environment in the system was estimated to be $\approx 0.2 T_C$.
[27] I. Giaever and K. Megerle, Phys. Rev. **122**, 1101 (1961).
[28] R. C. Bruno and B. B. Schwartz, Phys. Rev. B **8**, 3161 (1973).
[29] F. Aspen and A. M. Goldman, Phys. Rev. Lett. **43**, 307 (1979).
[30] P. Jalkanen, V. Tubolstev, A. Virtanen, K. Arutyunov, J. Räisänen, O. Lebedev, and G. V. Tendeloo, Solid State Commun. **142**, 407 (2007).